Metagratings: Beyond the Limits of Graded Metasurfaces for Wave Front Control

Younes Ra'di, Dimitrios L. Sounas, and Andrea Alù*
Department of Electrical and Computer Engineering, The University of Texas at Austin, Austin, Texas 78712, USA
(Received 8 May 2017; published 10 August 2017)

Graded metasurfaces exploit the local momentum imparted by an impedance gradient to mold the impinging wave front. This approach suffers from fundamental limits on the overall conversion efficiency, and it is challenged by fabrication limitations on the spatial resolution. Here, we introduce the concept of metagratings, formed by periodic arrays of carefully tailored bianisotropic inclusions and show that they enable wave front engineering with unitary efficiency and significantly lower fabrication demands. We employ this concept to design reflective metasurfaces for wave front steering without limitations on efficiency. A similar approach can be extended to transmitted beams and arbitrary wave front transformation, opening opportunities for highly efficient metasurfaces for extreme wave manipulation.

DOI: 10.1103/PhysRevLett.119.067404

Metasurfaces are thin structured arrays that have attracted significant attention for the level of control of electromagnetic waves that they enable [1–6]. In particular, phase-gradient metasurfaces have been explored to tailor the electromagnetic wave front to realize low-profile lenses, holograms, beam steerers, and other ultrathin optical devices. The majority of these geometries have been based on the generalized laws of reflection and refraction [7], based on which we can engineer the local reflection and/or transmission coefficients so that the impinging wave acquires the tangential momentum necessary to be locally rerouted towards the desired direction [7–17]. As research in this area has progressed, a few papers [18–20] have pointed out how this approach is inherently limited in efficiency, especially when extreme wave manipulation is considered. For instance, in the canonical problem of plane wave steering, it has been realized that the phase-gradient approach fundamentally suffers from a trade-off between efficiency and steering angle. Since this design method does not take into account the impedance mismatch between impinging and desired wave fronts, a dramatic reduction of efficiency and an increase of scattering to spurious directions is expected as the steering angle increases, even in the ideal limit in which we are able to engineer the desired phase profile with infinite resolution. Considering also fabrication limitations, these inefficiencies grow larger. These issues have important implications in the design of metasurfaces for extreme wave transformations, beyond what commonly achievable with conventional gratings [21–22].

These inherent limitations of phase-gradient metasurfaces can be overcome by designing metasurfaces with a surface impedance profile determined by the exact boundary conditions for the local impinging and scattered electromagnetic fields, which include impedance matching considerations. Based on this approach, however, transforming an incident wave towards an arbitrary direction with unitary efficiency in general requires locally active or strongly nonlocal metasurfaces [18–19]. Exploiting the interference with evanescent [23] or leaky [24–25] modes, passive impedance profiles can emulate the required nonlocal effects and get close to unitary efficiency. Such metasurfaces, however, are still subject to implementation difficulties when the limited fabrication resolution is considered, since they also require the discretization of a continuous, fastly varying impedance profile.

Here, we introduce a different route to the design of metasurfaces for arbitrary wave front transformation, which we call *metagratings*, enabling unitary efficiency without the need of deeply subwavelength elements, turning away from the discretization of a continuous phase or impedance profile. We exploit the physics of a grating, in which the local period selects a discrete set of diffraction orders, and enrich its wave control by considering complex metamaterial scatterers as the elements forming the grating. As we prove in the following, the scatterers can be designed to suppress undesired diffraction orders and reroute the incident power towards the desired ones with unitary efficiency. Since we do not focus on discretizing a continuous phase or impedance profile, the metasurface does not require subwavelength resolution, and the typical sizes of the involved elements are in the order of the wavelength of excitation.

In the following, we focus on the challenging problem of beam steering in reflection with unitary efficiency, which is not possible without relying on active metasurfaces or on nonlocal effects if we consider continuous impedance profiles [18]. Recent works have shown that passive metasurfaces can ensure large steering efficiency by relying on nonlocal effects stemming from the excitation of evanescent [23] or leaky modes [24], but this typically leads to complex design requirements and deeply subwavelength fabrication resolution. Interestingly, here we prove that a suitably tailored individual scatterer per unit cell is sufficient to enable highly complex diffraction scenarios of

significant practical interest, with unitary efficiency. We then explore the physical mechanism behind this anomalous diffraction and discuss the extension of the proposed approach to other scenarios of practical interest.

Consider first the basic geometry of an array of horizontally oriented magnetically polarizable particles located at a distance h from a ground plane [see Fig. 1(a)].

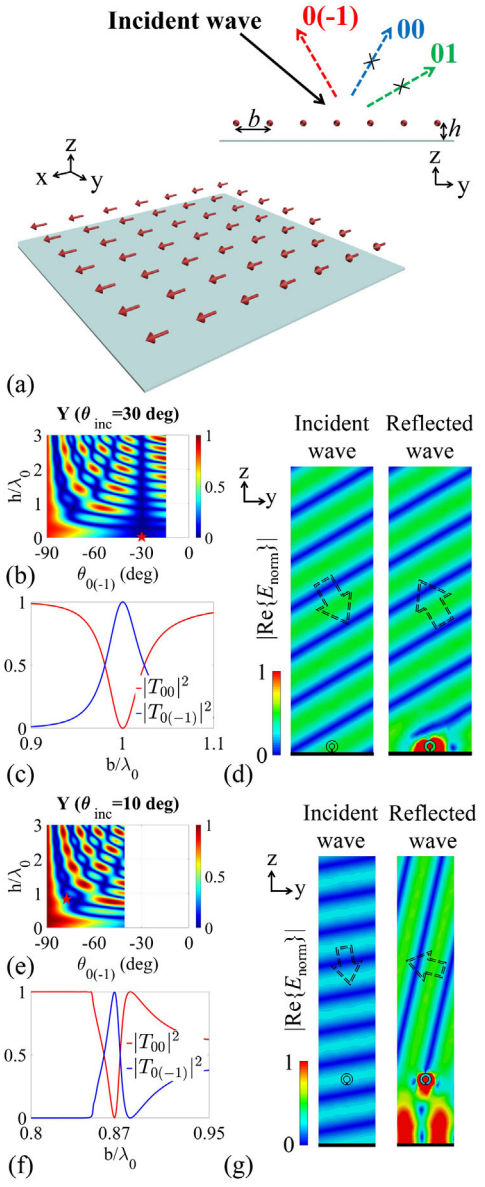

FIG. 1. (a) Array of horizontal magnetically polarizable particles located over a ground plane. (b) Magnitude of $Y = \cos\theta_{0(-1)}\cos^2(k_{z00}h) - \cos\theta_{00}\cos^2(k_{z0(-1)}h)$, whose zeros correspond to the solutions of Eq. (4), for different design parameters, and $\theta_{\rm inc} = 30$ deg. Dark blue areas correspond to parameters that satisfy Eq. (4), white areas to regions that support propagating Floquet modes other than $0(-1)$. (c) Reflected power into 00 and $0(-1)$ Floquet modes versus normalized frequency for the geometry indicated by a star in panel b. (d) Distribution of incident and reflected electric fields at the design frequency, normalized to their maximum. (e,f,g) Similar, but for $\theta_{\rm inc} = 10$ deg.

We assume that the structure is illuminated with a transverse magnetic (TM) plane wave propagating in the yz plane with electric field $\mathbf{E}_{\rm inc} = E_0(\mathbf{y}\cos\theta_{\rm inc} + \mathbf{z}\sin\theta_{\rm inc})\times \exp(-jk_0\sin\theta_{\rm inc}y + jk_0\cos\theta_{\rm inc}z)$, where E_0 is its amplitude, k_0 is the free-space wave number, and $\theta_{\rm inc}$ is the incidence angle defined in the counterclockwise direction with respect to the z axis. The metasurface sustains an induced surface magnetic current density $\mathbf{J}_{\rm m}(x,y,z) = \mathbf{x}\, I^{\rm x}_{\rm m}\delta(z-h)\sum_{m=-\infty}^{\infty}\sum_{n=-\infty}^{\infty}\delta(x-ma)\delta(y-nb)\times \exp(-jk_{y0}nb)$, where $k_{y0} = k_0\sin\theta_{\rm inc}$, $\delta(x)$ is the Dirac's delta function, $I^{\rm x}_{\rm m}$ is the magnetic current on each dipole, and a, b are the periodicities in x and y directions. $I^{\rm x}_{\rm m} = j\omega\hat{\alpha}^{\rm xx}_{\rm mm}H^{\rm x}_{\rm ext}$, where $H^{\rm x}_{\rm ext}$ is the impinging magnetic field in the absence of the array and $\hat{\alpha}^{\rm xx}_{\rm mm}$ is the effective magnetic polarizability of the particles, defined in the presence of all other particles [26]. In absence of Ohmic loss or gain, the quantity $\hat{\alpha}^{\rm xx}_{\rm mm}$ satisfies the generalized passivity condition [27]

$$\mathrm{Im}\left(\frac{1}{\hat{\alpha}^{\rm xx}_{\rm mm}}\right) = \frac{\omega}{\eta_0 ab}\sum_{n\in\text{propagating}}\frac{1}{\cos\theta_{0n}}\cos^2(k_{z0n}h), \quad (1)$$

which stems from the fact that the total radiated power carried away from the metasurface through all Floquet modes equals the extinction power. Here, ω is the angular frequency, $k_{z0n} = k_0\cos\theta_{0n}$ is the wave number in the z direction of the $0n$ mode (the first and second indices are the Floquet orders with respect to the x and y axes), η_0 is the free-space wave impedance, and θ_{0n} is the corresponding direction angle. As a function of the period, the power is coupled to a discrete number of diffraction orders [28]. We select the period so that no higher-order modes can propagate due to the periodicity in the x direction. The radiated fields for the $0n$ mode can be written as $\mathbf{E}_{0n} = (\mathbf{y} - \mathbf{z}\,k_{y0n}/k_{z0n})Q_{0n}\exp(-jk_{y0n}y - jk_{z0n}z)$, where $Q_{0n} = I^{\rm x}_{\rm m}\cos(k_{z0n}h)/(ab)$ and $k_{y0n} = k_{y0} + 2n\pi/b = k_0\sin\theta_{0n}$ is the wave number in the y direction.

In order to fully transmit the incident wave to a direction different than the specular one, we design the period to align one of the higher-order Floquet modes to this desired angle. In order for all the incident power to be transferred to the $0(-1)$ mode, for instance, we need to make sure that the structure does not radiate power into the specular channel 00 and all other propagating higher-order channels. The direct reflection from the ground plane can be canceled by the 00 Floquet mode, which is achieved if $Q_{00} = E_0\cos\theta_{\rm inc}$, leading to the condition

$$\frac{1}{\hat{\alpha}^{\rm xx}_{\rm mm}} = j\omega\frac{2}{\eta_0 ab}\frac{1}{\cos\theta_{00}}\cos^2(k_{z00}h). \quad (2)$$

The required magnetic polarizability is purely imaginary, showing that cancellation of specular reflection happens at the metagrating resonance [26]. In addition to this cancellation, we need to make sure that all higher-order modes

other than $0(-1)$ do not carry power away from the metasurface, which is achieved by making sure that these modes are evanescent, under the conditions

$$\begin{aligned}\theta_{0(-1)} &< \arcsin(2\sin\theta_{\text{inc}} - 1), \quad \text{for } 0 < \theta_{\text{inc}} < \arcsin(\tfrac{1}{3}) \\ \theta_{0(-1)} &< \arcsin\left(\tfrac{1}{2}\sin\theta_{\text{inc}} - \tfrac{1}{2}\right), \quad \text{for } \arcsin(\tfrac{1}{3}) < \theta_{\text{inc}} < \tfrac{\pi}{2}\end{aligned}. \tag{3}$$

Comparing Eq. (2) with Eq. (1), we obtain the design equation

$$\frac{1}{\cos\theta_{00}}\cos^2(k_{z00}h) = \frac{1}{\cos\theta_{0(-1)}}\cos^2(k_{z0(-1)}h), \tag{4}$$

from which we can calculate the required distance of the magnetic dipoles from the ground plane.

Figure 1(b) shows the difference between right- and left-handed sides of Eq. (4) for different values of h and $\theta_{0(-1)}$, where $\theta_{\text{inc}} = 30$ deg. A zero corresponds to a solution for which the optimum polarizability can be found using Eq. (2). Interestingly, if the array of dipoles is located right on top of the ground plane ($h = 0$), the only available solution is retroreflection, i.e., $\theta_{0(-1)} = -\theta_{\text{inc}}$. Retroreflection with unitary efficiency can also be achieved for any other value of height h. As an example, in Figs. 1(c)–1(d), we show the response of a metasurface consisting of an array of magnetic dipoles located on the ground plane that provides unitary retroreflection (design point indicated by a star in panel b, and corresponding geometry described in [27]). In particular, panel (c) shows the dispersion of the transmission towards the two diffraction orders as a function of normalized wavelength, showing a moderately broad response in terms of frequency or parameter variations, while panel (d) shows the field distributions for the geometry enabling unitary efficiency at the design frequency. These results are in agreement with recent works demonstrating retroreflection with a large efficiency using passive metasurfaces [29–33]. However, as we show in the following, our approach can be directly extended to significantly more complex diffraction scenarios.

Consistent with Fig. 1(b), Fig. 1(e) shows that this basic geometry is capable of rerouting all the incident power to arbitrary desired directions by controlling the height h, with a large flexibility, independent of the incidence angle. As an extreme example, we show in Figs. 1(f)–1(g) similar results for an array of dipoles that reroutes an incident wave from $\theta_{\text{inc}} = 10$ deg to $\theta_{0(-1)} = -77$ deg (red star). Figures 1(f) and 1(g) present the power coupled into modes 00 and $0(-1)$, and the near-field distributions around this array, respectively, showing that the illuminated power can be entirely reflected back into the $0(-1)$ mode with unitary efficiency at the design frequency. By simply tailoring the distance from the ground plane, it is possible to reroute the incident wave into an extremely slanted direction, without having to worry about complex, fastly varying phase profiles.

In the results shown in Fig. 1, we used a wire loop with a gap (detailed geometry described in [27]); however, a similar response can be achieved with other geometries offering a magnetic response, for instance, with dielectric or metallic-dielectric nanoparticles at optical frequencies [34–36]. It is remarkable to notice how a single particle per unit cell, suitably placed at a specific distance from the reflector, can couple all the impinging energy to the desired, extreme angle. At a small distance above the particle, the local field impedance is exactly the one necessary to transform the impinging wave front to the desired one, but this can be achieved with a totally passive, single inclusion, exploiting the near-field interactions with the impinging wave. Figures 1(c) and 1(f) show the frequency response of the array, ensuring a moderately broadband response, considering the extreme wave manipulation for which the metasurface was designed. Less extreme beam steering enables broader frequency responses. The reason for this moderate broadband behavior is that the metasurfaces based on the proposed concept do not require subwavelength fabrication resolution, lifting the necessity of providing the required response using deeply subwavelength particles. This can relax the requirements on Q factor for the particle, which is typically a significant challenge in conventional metasurface approaches. Note that the single particle is slightly detuned from its individual resonance, due to the array coupling, as Eqs. (1)–(2) refer to the effective polarizability of the array, including the coupling with all other particles, which is not negligible especially as we design the particle with a size comparable to the metagrating period.

Up to this point, we studied the basic geometry of an array of magnetically polarizable particles located over a ground plane. In this case, we are limited in terms of θ_{inc} and $\theta_{0(-1)}$ by Eq. (3), which ensures that all Floquet modes with $n \neq \{0, -1\}$ are evanescent. The white areas in Figs. 1(b)–1(e) correspond to these forbidden regions. In addition, when both 01 and $0(-1)$ modes are propagating, this array does not have enough degrees of freedom to cancel one of these modes and reroute the entire incident wave to the other one. For example, with such a structure, we cannot achieve perfect diffraction efficiency for a normally incident wave ($\theta_{\text{inc}} = 0$) to another arbitrary angle, since in this scenario, both the $0(-1)$ and 01 Floquet modes are propagating. Physically, this is consistent with the fact that magnetic dipoles alone cannot break the symmetry of the array for normal incidence, implying that the $0(-1)$ and 01 modes would be excited with equal amplitude. In order to reroute the entire illuminated wave into one of these degenerate modes and cancel out the fields in the other one, we need inclusions that scatter asymmetrically for normal incidence, which may be achieved with bianisotropic particles with coupled electric and magnetic responses [37], as in Fig. 2(a).

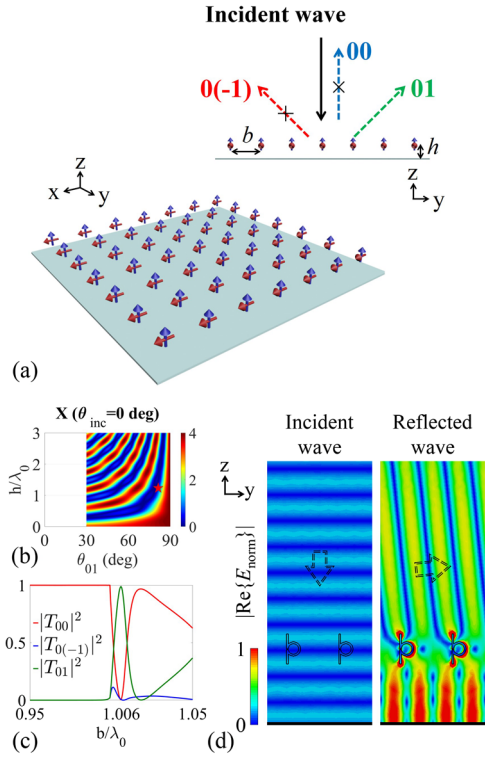

FIG. 2. (a) Array of bianisotropic omega particles located over a ground plane. (b) Similar to Fig. 1, magnitude of $X = \cos\theta_{01}\cos^2(k_0 h) - 4\cos^2(k_{z01} h)$ for $\theta_{inc} = 0$ deg. (c) Reflected power into 00, 0(−1), and 01 Floquet modes versus normalized frequency for the parameters indicated by the red star in (b) (detailed geometry in [27]). (d) Distribution of incident and reflected electric fields at the design frequency, normalized to their maximum.

Such particles provide the symmetry breaking required to suppress the additional propagating Floquet mode.

In this case, the unwanted diffraction orders can be suppressed as long as the array polarizabilities satisfy [27]

$$\frac{1}{\hat{\alpha}_{ee}^{zz}} = j\omega\frac{2\eta_0}{3ab}\sin^2\theta_{0(-1)}\cos^2(k_0 h),$$
$$\frac{1}{\hat{\alpha}_{mm}^{xx}} = j\omega\frac{2}{\eta_0 ab}\cos^2(k_0 h),$$
$$\frac{1}{\hat{\alpha}_{em}^{zx}} = -j\omega\frac{2}{ab}\sin\theta_{01}\cos^2(k_0 h). \quad (5)$$

These conditions, combined with the passivity condition [27] $\cos^2(k_0 h) = (4/\cos\theta_{01})\cos^2(k_{z01} h)$ and with the requirement that $0n$ higher-order Floquet modes with $|n| \geq 2$ are evanescent, enable steering a normally incident beam to an arbitrary angle θ_{01} larger than 30 deg. For $\theta_{01} < 30$ deg, Floquet modes with $|n| \geq 2$ also carry power, generally reducing the efficiency. In this case, more degrees of freedom, e.g., a second inclusion in each unit cell, would be required to achieve unitary efficiency.

As an example, we designed a metasurface based on omega bianisotropic particles that fully reflects a normally incident wave to $\theta_{01} = 83$ deg. An initial estimation for the design parameters can be obtained from Eq. (5) and the corresponding passivity condition [see solutions in Fig. 2(b)]. The geometry and design procedure of the bianisotropic omega particle are detailed in [27]. Figures 2(c)–2(d) present the frequency response of the structure and the fields at the design frequency, showing that all the illuminated power is transferred to the 01 harmonic. At optical frequencies, similar scattering responses may be achieved with dielectric nanoparticles with broken inversion symmetry [38], which also provide extremely low losses. In this extreme case of wave rerouting, while the efficiency is unitary, the bandwidth of operation is quite narrow. For less extreme designs or using more than one particle per unit cell, the bandwidth can be broadened.

More in general, here we have discussed the concept of metagrating, based on which we can use a conventional diffraction grating approach to select the desired channels in reflection, and then tailor the electromagnetic response of an individual complex inclusion within each unit cell to realize unitary efficiency for arbitrary wave front manipulation in a simple design that requires low spatial fabrication resolution. While here we focused on the case of reflective metasurfaces, the same concept can be extended to ideally manipulate transmitted wave fronts. For instance, by realizing two metasurfaces back to back with suitably tailored polarizabilities, it is possible to control reflection and transmission with unitary efficiency. Beyond beam steering, we envision that the proposed concept enables the realization of an ultralow profile, highly efficient planar lenses with short focal distances, all-angle absorbing or reflecting metasurfaces, holograms, and other wave transformations. Following this approach, we can create a large surface in which the period is locally modified to steer the beam in different directions, realizing focusing or holograms. A related approach has been recently followed to realize an efficient ultrathin focusing lens [39], but in this case, a few inclusions per unit cell were considered, and the efficiency was not unitary. Our Letter proves that it is not necessary to aim at implementing a local continuous phase and/or impedance profile within each unit cell of the metasurface to realize highly efficient wave front manipulation. Instead, a single, properly designed bianisotropic scatterer per unit cell is sufficient to realize unprecedented wave manipulation with efficiencies larger than what is allowed with conventional metasurface approaches. In this Letter, we focused on ideally lossless inclusions, in order to show that unbounded efficiency can be achieved following this approach. However, even considering realistic absorption, very large efficiencies can be expected, because the considered inclusions do not need to be deeply subwavelength, a feature that offers inherently more resilience to losses and reduced bandwidth constraints. The use of

multiple inclusions within each unit cell may be explored to further increase the bandwidth of operation, or to realize multifrequency, dual polarization, or low-aberration responses [40–41].

This work was supported by the Air Force Office of Scientific Research under Grant No. FA9550-17-1-0002, the National Science Foundation, the Simons Foundation, and the Welch Foundation with Grant No. F-1802.

*To whom correspondence should be addressed.
alu@mail.utexas.edu

[1] C. L. Holloway, E. F. Kuester, J. A. Gordon, J. O'Hara, J. Booth, and D. R. Smith, An overview of the theory and applications of metasurfaces: The two-dimensional equivalents of metamaterials, IEEE Trans. Antennas Propag. **54**, 10 (2012).
[2] C. Pfeiffer and A. Grbic, Metamaterial Huygens' Surfaces: Tailoring Wave Fronts with Reflectionless Sheets, Phys. Rev. Lett. **110**, 197401 (2013).
[3] Y. Zhao, X.-X. Liu, and A. Alù, Recent advances on optical metasurfaces, J. Opt. **16**, 123001 (2014).
[4] N. Yu and F. Capasso, Flat optics with designer metasurfaces, Nat. Mater. **13**, 139 (2014).
[5] S. A. Tretyakov, Metasurfaces for general transformations of electromagnetic fields, Phil. Trans. R. Soc. A **373**, 20140362 (2015).
[6] S. B. Glybovski, S. A. Tretyakov, P. A. Belov, Y. S. Kivshar, and C. R. Simovski, Metasurfaces: From microwaves to visible, Phys. Rep. **634**, 1 (2016).
[7] Na. Yu, P. Genevet, M. A. Kats, F. Aieta, J.-P. Tetienne, F. Capasso, and Z. Gaburro, Light propagation with phase discontinuities: Generalized laws of reflection and refraction, Science **334**, 333 (2011).
[8] A. V. Kildishev, A. Boltasseva, and V. M. Shalaev, Planar photonics with metasurfaces, Science **339**, 1232009 (2013).
[9] S. Sun, K.-Y. Yang, C.-M. Wang, T.-K. Juan, W. T. Chen, C. Y. Liao, Q. He, S. Xiao, W.-T. Kung, G.-Y. Guo, L. Zhou, and D. P. Tsai, High-efficiency broadband anomalous reflection by gradient meta-surfaces, Nano Lett. **12**, 6223 (2012).
[10] F. Monticone, N. M. Estakhri, and A. Alù, Full Control of Nanoscale Optical Transmission with a Composite Metascreen, Phys. Rev. Lett. **110**, 203903 (2013).
[11] A. Pors, M. G. Nielsen, R. L. Eriksen, and S. I. Bozhevolnyi, Broadband focusing flat mirrors based on plasmonic gradient metasurfaces, Nano Lett. **13**, 829 (2013).
[12] M. Esfandyarpour, E. C. Garnett, Y. Cui, M. D. McGehee, and M. L. Brongersma, Metamaterial mirrors in optoelectronic devices, Nat. Nanotechnol. **9**, 542 (2014).
[13] M. Kim, A. M. H. Wong, and G. V. Eleftheriades, Optical Huygens Metasurfaces with Independent Control of the Magnitude and Phase of the Local Reflection Coefficients, Phys. Rev. X **4**, 041042 (2014).
[14] Z. Bomzon, G. Biener, V. Kleiner, and E. Hasman, Space-variant Pancharatnam–Berry phase optical elements with computer-generated subwavelength gratings, Opt. Lett. **27**, 1141 (2002).
[15] E. Hasman, V. Kleiner, G. Biener, and A. Niv, Polarization dependent focusing lens by use of quantized Pancharatnam–Berry phase diffractive optics, Appl. Phys. Lett. **82**, 328 (2003).
[16] E. Hasman, Z. Bomzon, A. Niv, G. Biener, and V Kleiner, Polarization beam-splitters and optical switches based on space-variant computer-generated subwavelength quasi-periodic structures, Opt. Commun. **209**, 45 (2002).
[17] V. S. Asadchy, Y. Ra'di, J. Vehmas, and S. A. Tretyakov, Functional Metamirros Using Bianisotropic Elements, Phys. Rev. Lett. **114**, 095503 (2015).
[18] N. Mohammadi Estakhri and A. Alù, Wavefront Transformation with Gradient Metasurfaces, Phys. Rev. X **6**, 041008 (2016).
[19] V. S. Asadchy, M. Albooyeh, S. N. Tcvetkova, A. Díaz-Rubio, Y. Ra'di, and S. A. Tretyakov, Perfect control of reflection and refraction using spatially dispersive metasurfaces, Phys. Rev. B **94**, 075142 (2016).
[20] A. Epstein and G. V. Eleftheriades, Huygens' metasurfaces via the equivalence principle: Design and applications, JOSA B **33**, A31 (2016).
[21] E. Silberstein, P. Lalanne, J.-P. Hugonin, and Q. Cao, Use of grating theories in integrated optics, JOSA A **18**, 2865 (2001).
[22] P. Lalanne and P. Chavel, Metalenses at visible wavelengths: Past, present, perspectives, Laser Photonics Rev. **11**, 1600295 (2017).
[23] A. Epstein and G. V. Eleftheriades, Synthesis of Passive Lossless Metasurfaces Using Auxiliary Fields for Reflectionless Beam Splitting and Perfect Reflection, Phys. Rev. Lett. **117**, 256103 (2016).
[24] A. Díaz-Rubio, V. S. Asadchy, A. Elsakka, and S. A. Tretyakov, From the generalized reflection law to the realization of perfect anomalous reflectors, arXiv: 1609.08041.
[25] V. S. Asadchy, A. Wickberg, A. Díaz-Rubio, and M. Wegener, Eliminating scattering loss in anomalously reflecting optical metasurfaces, ACS Photonics **4**, 1264 (2017).
[26] S. A. Tretyakov, *Analytical Modeling in Applied Electromagnetics* (Artech House, Norwood, MA, 2003).
[27] See Supplemental Material at http://link.aps.org/supplemental/10.1103/PhysRevLett.119.067404 for the detailed analytical derivations of the required polarizabilities, design parameters, and information regarding the simulation setup.
[28] A. K. Bhattacharyya, *Phased Array Antennas: Floquet Analysis, Synthesis, BFNs and Active Array Systems* (Wiley, Hoboken, NJ, 2006).
[29] Z.-L. Deng, S. Zhang, and G. P. Wang, A facile grating approach towards broadband, wide-angle and high-efficiency holographic metasurfaces, Nanoscale **8**, 1588 (2016).
[30] X. Su, Z. Wei, C. Wu, Y. Long, and H. Li, Negative reflection from metal/graphene plasmonic gratings, Opt. Lett. **41**, 348 (2016).
[31] N. Mohammadi Estakhri, V. Neder, M. W. Knight, A. Polman, and A. Alù, Visible light, wide-angle graded metasurface for back reflection, ACS Photonics **4**, 228 (2017).
[32] D. L. Sounas, N. M. Estakhri, and A. Alù, Metasurfaces with Engineered Reflection and Transmission: Optimal

Designs Through Coupled-Mode Analysis, in 10th International Congress on Advanced Electro-magnetic Materials in Microwaves and Optics—Metamaterials 2016, Crete, Greece, 2016.

[33] M. Memarian, X. Li, Y. Morimoto, and T. Itoh, Wide-band/angle blazed surfaces using multiple coupled blazing resonances, Sci. Rep. **7**, 42286 (2017).

[34] J. C. Ginn, I. Brener, D. W. Peters, J. R. Wendt, J. O. Stevens, P. F. Hines, L. I. Basilio, L. K. Warne, J. F. Ihlefeld, P. G. Clem, and M. B. Sinclair, Realizing Optical Magnetism from Dielectric Metamaterials, Phys. Rev. Lett. **108**, 097402 (2012).

[35] M. R. Shcherbakov, D. N. Neshev, B. Hopkins, A. S. Shorokhov, I. Staude, E. V. Melik-Gaykazyan, M. Decker, A. A. Ezhov, A. E. Miroshnichenko, I. Brener, A. A. Fedyanin, and Y. S. Kivshar, Enhanced third-harmonic generation in silicon nanoparticles driven by magnetic response, Nano Lett. **14**, 6488 (2014).

[36] Y. Ra'di, V. S. Asadchy, S. U. Kosulnikov, M. M. Omelyanovich, D. Morits, A. V. Osipov, C. R. Simovski, and S. A. Tretyakov, Full light absorption in single arrays of spherical nanoparticles, ACS Photonics **2**, 653 (2015).

[37] A. N. Serdyukov, I. V. Semchenko, S. A. Tretyakov, and A. Sihvola, *Electromagnetics of Bi-Anisotropic Materials: Theory and Applications* (Gordon and Breach Science Publishers, Amsterdam, 2001).

[38] R. Alaee, M. Albooyeh, M. Yazdi, N. Komjani, C. Simovski, F. Lederer, and C. Rockstuhl, Magnetoelectric coupling in nonidentical plasmonic nanoparticles: Theory and applications, Phys. Rev. B **91**, 115119 (2015).

[39] R. Paniagua-Dominguez, Y. F. Yu, E. Khaidarov, R. M. Bakker, X. Liang, Y. H. Fu, and A. I. Kuznetsov, A metalens with near-unity numerical aperture, arXiv:1705.00895.

[40] F. Aieta, P. Genevet, M. A. Kats, N. Yu, R. Blanchard, Z. Gaburro, and F. Capasso, Aberration-free ultrathin flat lenses and axicons at telecom wavelengths based on plasmonic metasurfaces, Nano Lett. **12**, 4932 (2012).

[41] F. Aieta, M. A. Kats, P. Genevet, and F. Capasso, Multi-wavelength achromatic metasurfaces by dispersive phase compensation, Science **347**, 1342 (2015).